ChemComm

Accepted Manuscript

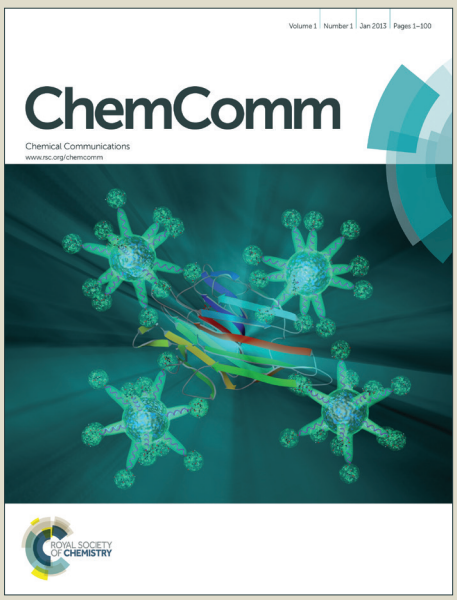

ROYAL SOCIETY OF CHEMISTRY

www.rsc.org/chemcomm

Journal Name

RSCPublishing

COMMUNICATION

The crosslink enhanced emission (CEE) in non-conjugated polymer dots: from photoluminescence mechanism to cellular uptake mechanism and internalization

Cite this: DOI: 10.1039/xoxxoooooox

Received ooth January 2012,
Accepted ooth January 2012

DOI: 10.1039/xoxxoooooox

www.rsc.org/

Shoujun Zhu,[a] Lei Wang,[b] Nan Zhou,[c] Xiaohuan Zhao,[a] Yubin Song,[a] Suraj Maharjan,[c] Junhu Zhang,[a] Laijin Lu,[c] Haiyu Wang,[b] and Bai Yang[a]*

The crosslink enhanced emission (CEE) in a new type of non-conjugated polymer dots (PDs) is proved. The enhanced PL originates from the decreased vibration and rotation of amino-based chromophore. Furthermore, the cellular uptake mechanism and internalization of PDs were investigated in detail.

Non-conjugated polymer dots (PDs), labeled as specific carbon dots (CDs),[1-4] possess aggregated polymer structures and have drawn increasingly attention in the last three years.[5-7] These kinds of PDs are different from the conjugated PDs, which are obtained from an assembly of fluorescent conjugated polymers.[8] The specific PDs are always prepared from the non-conjugated polymer by dehydration, condensation, carbonization or assembly routes.[9-14] In these situations, the PL centers are attributed to the formed carbon-core or the molecule/groups chromophore. Due to the convenient surface modification, the PDs are very promising as novel fluorescent materials.[15] To extend the applications of these kinds of materials, it is highly important to confirm a clear PL mechanism in such non-conjugated PDs.[16]

PL behaviors were investigated in polyvinyl alcohol PDs and polymer-like CDs.[7, 17, 18] In these kinds of materials, the forming of polymer aggregations (PDs) promoted the PL behavior. What's the relationship between the PL property and the aggregated chemical structure? To answer this question, herein, using branched polyethyleneimine (PEI) as model system, the PDs were prepared by carbon tetrachloride (CTC) crosslink. We found that the crosslink enhanced emission (CEE) effect in the PDs was the key factor in the PL of PDs. The enhanced PL originated from the decreased vibration and rotation of crosslinked PEI. Furthermore, the universality of crosslink enhanced PL was proved by other three kinds of crosslinked PDs. From the femtosecond broadband transient absorption (TA) spectroscopy analysis, the consistent excited state was observed in serials of PDs, which illustrated the same PL mechanism for these PDs. The present work developed a general and proof-of-concept rule on CEE for non-conjugated PDs. Moreover, the cellular uptake mechanism and internalization of PDs were investigated in detail, which gave a direction of applications for these kinds of materials.[19]

The Fig. S1 illustrates the preparation route of the crosslinked PDs. The initial materials are commercial branched PEI with ethylenediamine repeated unit. After CTC crosslinking, partial primary amine changed to secondary amine; partial secondary amine changed to tertiary amine; and partial tertiary amine changed to quaternary amine.[6] There are amine based molecule states (mainly secondary and tertiary amine) for PL centers in the PEI system,[20, 21] but the radiation recombination was confined, while the enhanced PL was supposed to be originated from the decreased vibration and rotation of the amine-based PL centers in crosslinked PEI dots.[22, 23]

The PDs possess a wide size distribution with average diameter ca. 63 nm (Fig. S2a-c), it was ca. 180 nm in average by dynamic light scattering (DLS). The chemical groups were determined by ^{1}H NMR (Fig. S3) and XPS analysis (Fig. S4). C1s analysis revealed that the percentage of C-N increased in the whole types of carbon atoms from the bare PEI to crosslinked PDs. There was a small formation of N-O in the PDs from N1s analysis, which was due to the surface oxidation of the PDs in the reaction process.[24] In the FTIR analysis of the PDs, the following chemical groups were observed and were the same as the initiative PEI: stretching vibrations of C-N at 3423 cm^{-1} and C-H at 2923 cm^{-1} and 2850 cm^{-1}, asymmetric stretching vibrations of C-N at 1126 cm^{-1}, bending vibrations of NH at 1615 cm^{-1} (Fig. S5).[25, 26] The zeta-potential of the PDs was ca. +9.8 mV due to the amino-based groups.

In the UV-Vis spectra, the wide peak was focused on ca. 350 nm in aqueous solution of PDs, and was assigned to n-π transition.[27] In the fluorescence spectra, PDs possess optimal excitation and emission wavelengths at 400 nm and 475 nm, and showed cyan color under a hand-held UV lamp (Fig. 1a). Excitation-dependent PL behaviors were observed, which are common in fluorescent carbon materials.[28] This behavior is contributed to the different molecule states in the PDs (Fig. 1b). Fortunately, the excitation-dependent PL behaviors can be applied in multi-color imaging applications (Fig. S6c-f). The PL was kept in dried samples (Fig. S6a-b), which attributed to polymer skeleton preventing the re-absorption effect of

the PL centers. Furthermore, the quantum yields of PDs reached 2.7% using quinine sulfate as a reference, and was notably better than the beginnig PEI (Fig. S7 and Table S1). Due the stable PL in solid state, the PDs can be applied as nanocomposite (Fig. S6g-h) and fluorescent inks (Fig. S8).

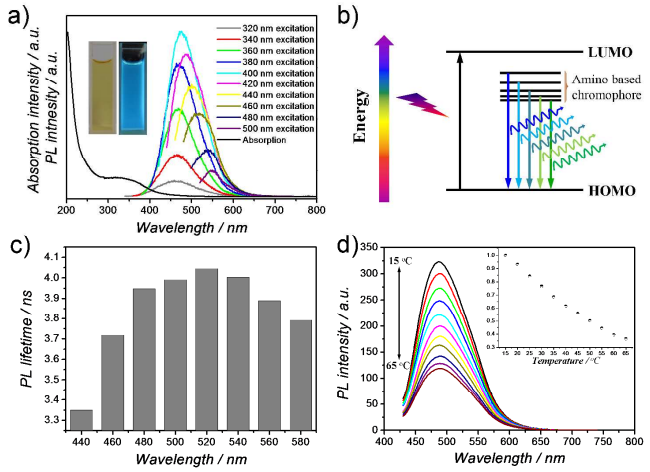

Fig. 1. The optical properties of PDs. a) The absorption and fluorescence spectra of PDs. The inset pictures were PDs aqueous solution under daylight and UV light excitation. b) The suggested excited level for PDs with excitation dependent behaviors. c) The PL lifetime of the PDs. d) The temperature dependent PL of PDs.

The decay time of PDs was about 3.35-4.05 ns probed from 440 to 580 nm, which contained two nanosecond components (Fig. 1c and Table S2). The PDs possessed temperature-dependent PL, with high temperature able to quench the PL to some degree (Fig. 1d). This behavior preliminary proved that the crosslinked skeleton decreased the vibration and rotation of the amine-based PL center in the PDs (the high temprature aggravated the vibration and rotation and increased the nonradiative process). The crosslinked amine-based PL center can be partial destroyed by high power UV excitation (Fig. S9). Although the steady PL decreased 38% after 20 min UV exposure, the PL lifetime increased 30%. It was possible that radiative process decreased due to partial crosslinking PDs degraded while the nonradiative process increased.[29]

To further illuminate the crosslink effect in enhancing the PL properties for this kind of linear polymer, three other PDs were prepared for further comparison. The above-mentioned PDs were named as PD 1; the PD 2 was prepared by PEI hydrothermal; the PD 3 was synthesized by connecting the PEI on the surface of the amorphous carbon dots; the PD 4 was synthesized by connecting the PEI on the surface of the carbon quantum dots. All of the PDs shared a common feature in that the PEI chains were immobilized to decrease the vibration and rotation of the amine-based PL centers (Fig. S10-11, Table S4).

Similar to the PD 1, PD 2 and 3 possess the absorption peak at ca. 350 nm and excitation-dependent PL behaviors (Fig. S12a-d). Due to the influence of the carbon core structure, the absorption and fluorescence spectra of PD 4 were slightly different with the PD 1-3 (Fig. S12e-f). The quantum yields were 2.7 %, 3.2%, 9.6 % and 0.5% for PD 1-4, respectively (Table S1). Furthermore, the PL lifetime of the PD 1-4 possess the similar trend compared with the quantum yield (Fig. 2a). Generally, a fluorophore is excited by a photon and will then the excited electron drop to the ground state with a certain probability. The probability is based on the decay rates through a number of different (radiative and/or nonradiative) decay pathways.

$$\tau = \frac{1}{k} = \frac{1}{k_F + \sum k_i} \qquad (1)$$

τ is the fluorescence lifetime, k is the total decay rate, k_F is the rate for radiative decay, k_i is the rate for nonradiative decay. In this system, the lifetime of bare PEI is mainly controlled by the nonradiative decay pathway (vibration and rotation process). For PD 1-3, the lifetime was mainly controlled by the radiative decay pathway. For PD 4, although the carbon core immobilized the PEI chains, the carbon core with multi-layer crystal lattice possessed non-radiative structures and traps. As a result, energy traps in carbon cores neutralized the enhanced PL of PEI coating.

Fig. 2. The excited behaviors of PDs. a) The average PL lifetime of bare PEI and PDs at different probed wavelength (380 nm excitation). b-e) Transient spectra of PD 1-4. f) The normalized TA dynamics probed at 475 nm for PD 1-4.

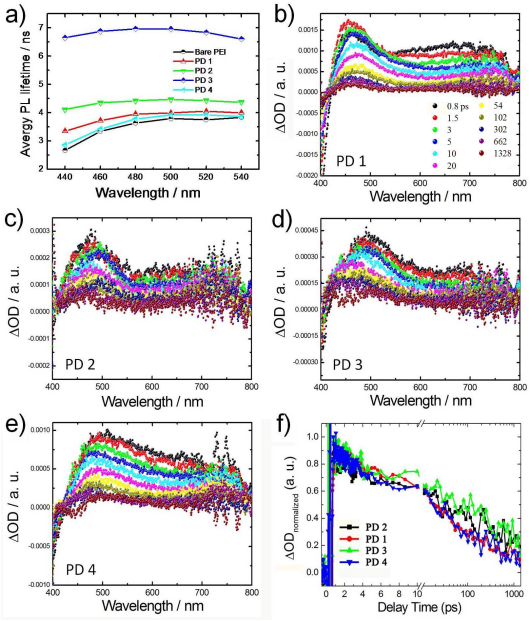

To gain more insight into the origin of the PL behavior of the PDs, femtosecond transient absorption (TA) spectroscopy was performed (Fig. 2b-e). All the features in TA reflect the information about the change of photogenerated carrier populations in corresponding energy levels.[30, 31] It is not any contribution to the transient signals for bare PEI molecules (Fig. S13). But for PD 1-4, the similar excited-state behaviors (same excited-state absorption (ESA)) reveal that all the PDs possess the same PL centers (Fig. 2b-e), no matter if they are synthesized by small molecule crosslinking, hydrothermal aggregation, or immobiled on the carbon core. This is further confirmed by the same normalized TA dynamics probed at their PL peaks of 475 nm (Fig. 2f).

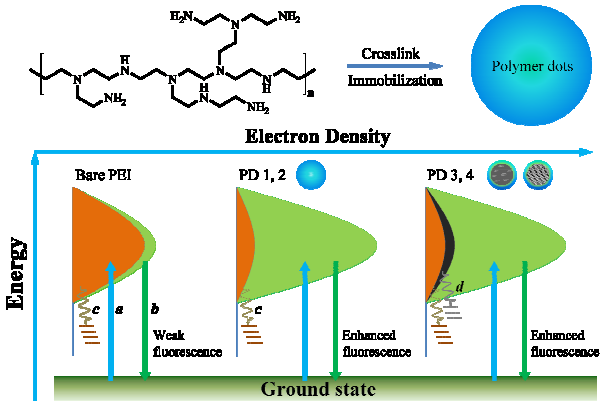

Fig. 3. Representation for the PL mechanism (CEE effect) of bare PEI and PD 1-4. a) Electrons excited from the ground state and trapped by the amino-based states; b) excited electrons return to the ground state via radiative route; c) excited electrons return to the ground state via a vibration and rotation non-radiative route; d) excited electrons return to the ground state via a carbon core-based non-radiative route.

According to the above mentioned analysis, the electron level of PEI and PEI PDs was described in Fig. 3 and S14. For bare PEI, the excited electrons mainly drop to the ground state through nonradiative vibration/rotation process. For PD 1 and 2, due the crosslinking skeleton, the vibration and rotation of the amino-based fluorophore were restricted, the percentage of radiative process increased (CEE effect). For PD 3, the PEI chains were immobilized by the amorphous carbon core, both the immobilization of PEI chains and the antenna effect of the carbon core enhanced the PL property; for PD 4, although the PEI chains were fixed and the amine-based center was enhanced by the CEE effect, the carbon core with multi-layer crystal lattice possessed non-radiative structures and traps (such as interlayer quenching). As a result, the CEE effect was neutralized by the non-radiative process, the radiative process was affected and confined.

Although the bioimaging applications were achieved by some kinds of CDs, there have been very few reports on investigating the cellular uptake mechanism and internalization.[2, 32] In vitro cytotoxicity of different PDs contents was evaluated with differentiated rat adrenal pheochromocytoma cells (PC12) by methylthiazolyldiphenyl-tetrazolium bromide (MTT) assay (Fig. 4c). Results suggest that PDs have a relative low toxicity to PC12 cells, with relative cell viability higher than 80% with 20-30 μg of PDs added. From Fig. 4a-b, the time-dependent uptake behavior of PDs was proved by both confocal laser scanning microscope (CLSM) and fluorescence activated cell sorter (FACS).

Due to the energy dependent effect, the complete endocytosis of PDs was proved by being suppressed at low temperature (4 °C instead of 37 °C) or in ATP-depleted environments (Fig. 4d).[33] The endocytosis pathways of PDs were further investigated by the addition of pharmacological inhibitors (Fig. 4d). Firstly, the inhibitors for caveolae-mediated endocytosis, genistein (a tyrosine kinase inhibitor and blocked the phosphorylation of caveolin-1) were used.[34] Compared to the normal cellular uptake of PDs at 37 °C, the uptake rates of PDs treated with genistein were reduced by ca. 50%. Thus, the significant decrease of PDs uptake indicated that caveolae-mediated endocytosis was one of the uptake pathways. Secondly, the inhibitor for clathrin-mediated endocytosis, chlorpromazine (CPZ), was used,[34] ca. 25% of the uptake inhibition rate were observed; demonstrating clathrin-mediated endocytosis also played a critical role in the uptake of PDs in PC12. Thirdly, the inhibitors for macropinocytosis were used CytoD (inhibiting F-actin polymerization) to suppress the macropinocytosis.[35] About 15% of the uptake inhibition rate was observed. Therefore, we concluded that PDs was internalized *via* caveolae-, clathrin- and macropinocytosis- mediated endocytosis in PC12 cells.

We further investigated the intracellular distribution of PDs by co-localizing with specific dyes of cell organelles in PC12 cells: propidium iodide (PI), LysoTracker red, ER-Tracker red and MitoTracker red were used to label nucleus, lysosomes, endoplasmic reticulum and mitochondria, respectively. The PDs was proved to be mainly distributed in the cytoplasm (Fig. 4e-h). Additionally, the intracellular distribution of PDs in PC12 cells was further confirmed using fixed slice TEM. As shown in Fig. 4i-k, a typical endocytosis process was observed at different culture stages, and PDs were wrapped by the formed vacuolar at 2 h culturing. The similar endocytosis and intracellular distribution of PDs have also proved in RSC96 cells (Fig. S15-16). Moreover, the PDs possessed high photostability compared with commercial dyes, which was proved by long time excitation by CLSM (Fig. S17).

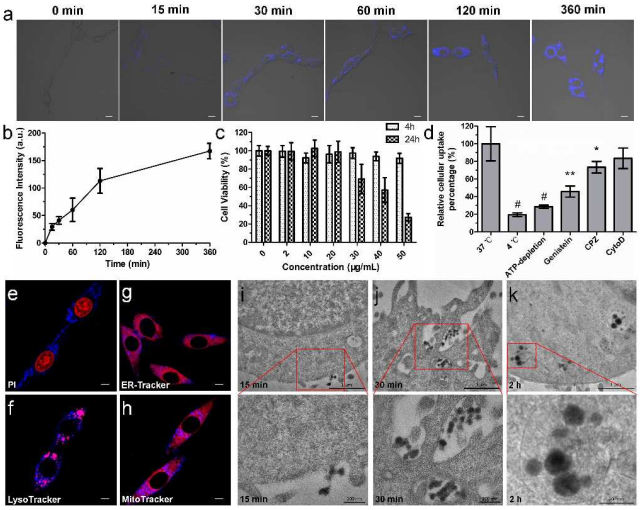

Fig. 4. The cellular (PC12 cells) uptake mechanism and internalization of PDs. a) The time-dependent cellular uptake of passivated PDs determined by CLSM (The scale bar is 10 μm). b) The time-dependent cellular uptake of PDs by FACS. c) Cytotoxicity of PDs. d) The FACS quantitative data for the uptake of PDs by PC12 cells incubated at 37 °C, 4 °C, ATP-depletion, inhibitors Genistein, chlorpromazine and cyto D treatments, respectively. e-h) PDs co-localized with cellular organelles specific dyes in PC12 cells. Propidium iodide (PI), LysoTracker red, ER-Tracker red and MitoTracker red were used to label nucleus, lysosomes, endoplasmic reticulum and mitochondria, respectively. The scale bar is 5 μm. i-k) The endocytotic process of PDs entering cell was detected by fixed slice TEM. The scale bar is 1 μm for upper images and 200 nm for nether images.

In summary, using branched polyethyleneimine (PEI) as a model non-conjugated polymer, the clear crosslink enhanced emission (CEE) was investigated by series of PDs. The enhanced PL originated from the decreased vibration and rotation of crosslinked PEI. The present work developed a general and proof-of-concept rule in crosslink enhanced PL for non-conjugated PDs. The reported

PDs are also kinds of special carbon dots (CDs) and as a result, they could be the model system to understand the relationship between the chemical structures and PL mechanism in these kinds of CDs. It should be noted that the suggested CEE was different from the reported aggregation-induced emission (AIE), which was mainly applied in small organic molecules.[36] Furthermore, we investigated the bioimaging applications of the PDs and proved the endocytosis route of the PDs entering into the cells.

S. Zhu and L. Wang contributed equally to this work. This work was supported by the National Science Foundation of China (Grand No. 51373065, 21221063, 81320108011, 91123031).

Notes and references

[a] *State Key Laboratory of Supramolecular Structure and Materials, College of Chemistry, Jilin University*
Changchun, 130012, P. R. China
E-mail: byangchem@jlu.edu.cn
[b] *State Key Laboratory on Integrated Optoelectronics, College of Electronic Science and Engineering, Jilin University*
Changchun, 130012, P. R. China
[c] *Department of Hand Surgery, the First Hospital of Jilin University*
Changchun, 130021, P.R. China

Electronic Supplementary Information (ESI) available: See DOI: 10.1039/c000000x/

1. L. Cao, M. J. Meziani, S. Sahu and Y. P. Sun, *Accounts of chemical research*, 2013, **46**, 171.
2. H. Li, Z. Kang, Y. Liu and S.-T. Lee, *Journal of Materials Chemistry*, 2012, **22**, 24230.
3. Y. Song, S. Zhu and B. Yang, *RSC Advances*, 2014, **4**, 27184.
4. S. Zhu, S. Tang, J. Zhang and B. Yang, *Chemical communications*, 2012, **48**, 4527.
5. S. Liu, J. Tian, L. Wang, Y. Zhang, X. Qin, Y. Luo, A. M. Asiri, A. O. Al-Youbi and X. Sun, *Advanced materials*, 2012, **24**, 2037.
6. Z. A. Qiao, Q. Huo, M. Chi, G. M. Veith, A. J. Binder and S. Dai, *Advanced materials*, 2012, **24**, 6017.
7. S. Zhu, J. Zhang, L. Wang, Y. Song, G. Zhang, H. Wang and B. Yang, *Chemical communications*, 2012, **48**, 10889.
8. C. Wu and D. T. Chiu, *Angewandte Chemie*, 2013, **52**, 3086.
9. K. Li, W. Qin, D. Ding, N. Tomczak, J. Geng, R. Liu, J. Liu, X. Zhang, H. Liu, B. Liu and B. Z. Tang, *Scientific reports*, 2013, **3**, 1150.
10. C. X. Guo, J. Xie, B. Wang, X. Zheng, H. B. Yang and C. M. Li, *Scientific reports*, 2013, **3**, 2957.
11. Y. Sun, W. Cao, S. Li, S. Jin, K. Hu, L. Hu, Y. Huang, X. Gao, Y. Wu and X. J. Liang, *Scientific reports*, 2013, **3**, 3036.
12. D. Ding, C. C. Goh, G. Feng, Z. Zhao, J. Liu, R. Liu, N. Tomczak, J. Geng, B. Z. Tang, L. G. Ng and B. Liu, *Advanced materials*, 2013, **25**, 6083.
13. X. Feng, J. Wu, M. Ai, W. Pisula, L. Zhi, J. P. Rabe and K. Mullen, *Angewandte Chemie*, 2007, **46**, 3033.
14. S. Zhu, L. Wang, B. Li, Y. Song, X. Zhao, G. Zhang, S. Zhang, S. Lu, J. Zhang, H. Wang, H. Sun and B. Yang, *Carbon*, 2014, **77**, 462.
15. P. Yang, Y. Zhao, Y. Lu, Q. Z. Xu, X. W. Xu, L. Dong and S. H. Yu, *ACS nano*, 2011, **5**, 2147.
16. Y. Yang, J. Cui, M. Zheng, C. Hu, S. Tan, Y. Xiao, Q. Yang and Y. Liu, *Chemical communications*, 2012, **48**, 380.
17. S. Zhu, Q. Meng, L. Wang, J. Zhang, Y. Song, H. Jin, K. Zhang, H. Sun, H. Wang and B. Yang, *Angewandte Chemie*, 2013, **52**, 3953.
18. Y. Song, S. Zhu, S. Xiang, X. Zhao, J. Zhang, H. Zhang, Y. Fu and B. Yang, *Nanoscale*, 2014, **6**, 4676.
19. S. Zhu, J. Zhang, Y. Song, G. Zhang, H. Zhang and B. Yang, *Acta Chimica Sinica*, 2012, **70**, 2311.
20. M. Sun, C. Y. Hong and C. Y. Pan, *Journal of the American Chemical Society*, 2012, **134**, 20581.
21. L. Pastor-Pérez, Y. Chen, Z. Shen, A. Lahoz and S.-E. Stiriba, *Macromolecular Rapid Communications*, 2007, **28**, 1404.
22. S. Maiti, K. Das and P. K. Das, *Chemical communications*, 2013, **49**, 8851.
23. M. J. Krysmann, A. Kelarakis, P. Dallas and E. P. Giannelis, *Journal of the American Chemical Society*, 2012, **134**, 747.
24. Z. Lin, W. Xue, H. Chen and J. M. Lin, *Chemical communications*, 2012, **48**, 1051.
25. Y. Mao, Y. Bao, D. Han, F. Li and L. Niu, *Biosensors & bioelectronics*, 2012, **38**, 55.
26. S. Zhu, J. Zhang, S. Tang, C. Qiao, L. Wang, H. Wang, X. Liu, B. Li, Y. Li, W. Yu, X. Wang, H. Sun and B. Yang, *Advanced Functional Materials*, 2012, **22**, 4732.
27. G. S. Kumar, R. Roy, D. Sen, U. K. Ghorai, R. Thapa, N. Mazumder, S. Saha and K. K. Chattopadhyay, *Nanoscale*, 2014, **6**, 3384.
28. Z. Zhang, J. Zhang, N. Chen and L. Qu, *Energy & Environmental Science*, 2012, **5**, 8869.
29. H. Sun, L. Wu, N. Gao, J. Ren and X. Qu, *ACS applied materials & interfaces*, 2013, **5**, 1174.
30. L. Wang, S. J. Zhu, H. Y. Wang, S. N. Qu, Y. L. Zhang, J. H. Zhang, Q. D. Chen, H. L. Xu, W. Han, B. Yang and H. B. Sun, *ACS nano*, 2014, **8**, 2541.
31. L. Wang, H. Y. Wang, Y. Wang, S. J. Zhu, Y. L. Zhang, J. H. Zhang, Q. D. Chen, W. Han, H. L. Xu, B. Yang and H. B. Sun, *Advanced materials*, 2013, **25**, 6539.
32. S. Zhu, J. Zhang, C. Qiao, S. Tang, Y. Li, W. Yuan, B. Li, L. Tian, F. Liu, R. Hu, H. Gao, H. Wei, H. Zhang, H. Sun and B. Yang, *Chemical communications*, 2011, **47**, 6858.
33. V. Mailander and K. Landfester, *Biomacromolecules*, 2009, **10**, 2379.
34. C. Y. Hsu and H. Uludag, *Biomaterials*, 2012, **33**, 7834.
35. X. Jiang, C. Rocker, M. Hafner, S. Brandholt, R. M. Dorlich and G. U. Nienhaus, *ACS nano*, 2010, **4**, 6787.
36. Y. Hong, J. W. Lam and B. Z. Tang, *Chemical Society reviews*, 2011, **40**, 5361.

The crosslink enhanced emission (CEE) in a new type of non-conjugated polymer dots (PDs) is reported. The enhanced PL originates from the decreased vibration and rotation of crosslinked PDs. The present work develops a general and proof-of-concept rule in crosslinking enhanced PL for non-conjugated PDs. Furthermore, the cellular uptake mechanism and internalization of PDs were investigated in detail.